

Guided Image Filter Using Multi-Exposure Image Fusion: A Patch-Wise Approach

Nalam Lavanya, DECS, Vikas Group of Institutions, Nunna, Vijayawada

P. Balakrishna, Asst Prof., Vikas Group of Institutions, Nunna, Vijayawada

S. Kishore Babu M.Tech(Ph.D), Vikas Group of Institutions, Nunna, Vijayawada

ABSTRACT:

A lot of research has been contributed in the area of optimization of design. MOST applications in computer vision and computer graphics involve image filtering to suppress and/or extract content in images. We propose a patch-wise approach for multi-exposure image fusion (MEF) using guided image filter. A key step in our approach is to decompose each colour image patch into three conceptually independent components: signal strength, signal structure and mean intensity. Upon processing the three components separately based on patch strength and exposedness measures, we uniquely reconstruct a colour image patch and place it back into the fused image. Unlike most pixel-wise MEF methods in the literature, the proposed algorithm does not require significant pre/post processing steps to improve visual quality or to reduce spatial artefacts. Moreover, the novel patch decomposition allows us to handle RGB colour channels jointly and thus produces fused images with more vivid colour appearances using guided image filter. Extensive experiments demonstrate the superiority of the proposed algorithm both qualitatively and quantitatively with guided filter. Hybrid thresholding is applied on remaining sub bands (LH, HL and HH). The proposed work will be implemented using MATLAB R2015a.

Index Terms— Multi-exposure fusion, image enhancement, perceptual image processing guided image filter.

1. INTRODUCTION

Natural scenes often contain luminance levels that span a very high dynamic range (HDR), whose visual information may not be fully captured by a normal camera with a fixed exposure Setting [1]. Multi-exposure image fusion (MEF) alleviates the problem by taking multiple images of the same scene under different exposure levels and synthesizing a low dynamic range (LDR) image from them. The resulting fused image is expected to be more informative and perceptually appealing than any of the input images. An example is given in Fig. 1. Compared with the typical HDR imaging pipeline, MEF bypasses the intermediate HDR construction step and directly yields an LDR image for normal displays.



(a) Source image sequence by courtesy of Erik Reinhard



(b) Song12 [2]

(c) Proposed

Fig. 1. Demonstration of MEF.

Intensity values at the i -th pixel in the k -th exposure image, respectively represents the fused image. A straightforward extension of this approach in transform domain is to replace $X_k(i)$ with transform coefficients. The weight map W_k often bears information regarding structure preservation and visual importance of the k -th input image at a pixel level. With specific models to quantify this information, existing MEF algorithms differ mainly in the computation of W_k . In 1994, Burt and applied pyramid decomposition [3] to MEF, where W_k is computed from local coefficient energy and the correlation between pyramids [4]. Martens et al. [5] defined contrast, colour saturation and well exposure measures to compute. The fusion is done in a multire solution fashion. Edge preserving filters such as bilateral filter [6], guided filter [7] and recursive filter [8] are applied to retrieve edge information and/or refine W_k in [9], [10] and [11] respectively. Song et al. [2] incorporated MEF into a MAP framework by first estimating the initial image with the maximum visual contrast and scene gradient, and then suppressing reversals in image gradients. Another MAP based approach embedded perceived local contrast and colour saturation [12]. Gu et al. [13] extracted pixel-level gradient information from the structure tensor and smoothed it to compute W_k . A similar gradient-based MEF method is proposed in [14]. By exploiting the gradient direction, the method is able to handle dynamic scenes that have moving objects.

In the image de-noising process, information about the type of noise present in the original image plays a significant role. De-noising of electronically distorted images is an old, there are many different cases of distortions. One of the most prevalent cases is distortion due to noise. Typical images are corrupted with noise modelled with either a Gaussian, uniform, Rician, or salt and pepper distribution. Another typical noise is a speckle noise, which is multiplicative in nature. Speckle noise is observed in ultrasound images, whereas Rician noise affects MRI images. Mostly, noise in digital images is found to be additive in nature with uniform power in the whole bandwidth and with Gaussian probability distribution. Such a noise is referred to as Additive White Gaussian Noise (AWGN). White Gaussian noise can be caused by poor image acquisition or by transferring the image data in noisy communication channel. Most de-noising algorithms use images artificially distorted with well-defined white Gaussian noise to achieve objective test results.

2. PATCH-WISE MULTI-EXPOSURE FUSION

Let $f_{xkj} = f_{xkj} | 1 < k < K$ be a set of colour image patches extracted from the same spatial location of the source sequence that contains K multi-exposure images. Here x_k for all k are column vectors of CN_2 dimensions, where C is the number of colour channels in the input images and N is the spatial size of a patch. Each entry of the vector is given by one of the

three intensity values in RGB channels of a pixel in the patch. Given any colour patch, we first decompose it into three components: signal strength, signal structure and mean intensity

We extract patches from the source sequence using a moving window with a fixed stride D . The pixels in overlapping patches are averaged to produce the final output. Throughout the paper, we set the patch size $N = 11$, the stride of moving window $D = n/2$ the exponent parameter

$p = 4$, two spreads of Gaussian profile $_g = 0.2$ and $_l = 0.5$. Empirically, we find that the proposed algorithm is robust to variations of N and p , and a smaller value of $_g$ relative to $_l$ is important to produce more perceptually appealing results. The proposed method can be applied to gray scale images simply by setting $C = 1$.

3. GUIDED IMAGE FILTER

We first define a general linear translation-variant filtering process, which involves a guidance image I , an input image p , and an output image q . Both I and p are given beforehand according to the application, and they can be identical. The filtering output at a pixel i is expressed as a weighted average:

$$q_i = \sum_j W_{ij} p_j, \text{----- (1)}$$

Where i and j are pixel indexes. The filter kernel W_{ij} is a function of the guidance image I and independent of p . This filter is linear with respect to p . A concrete example of such

a filter is the joint bilateral filter [11]. The bilateral filtering kernel W_{bf} is given by:

$$W_{bf}(ij) = 1/K_i \exp(-|x_i - x_j|^2 / \sigma_s^2) \exp(-|I_i - I_j|^2 / \sigma_r^2), \text{----- (2)}$$

Where x is the pixel coordinate, and K_i is a normalizing parameter to ensure that $\sum_j W_{bf}(ij) = 1$. The parameters σ_s and σ_r adjust the spatial similarity and the range (intensity/colour) similarity respectively. The joint bilateral filter degrades to the original bilateral filter [1] when I and p are identical.

3.1 DEFINITION

Now we define the guided filter and its kernel. The key assumption of the guided filter is a local linear model between the guidance I and the filter output q . We assume that q is a linear transform of I in a window ω_k centred at the pixel k :

$$q_i = a_k I_i + b_k, \forall i \in \omega_k, \text{----- (3)}$$

Where (a_k, b_k) are some linear coefficients assumed to be constant in ω_k . We use a square window of a radius r . This local linear model ensures that q has an edge only if I has an edge, because $\nabla q = a \nabla I$. This model has been proven useful in image matting [2], image super-resolution [26], and haze removal [9]. To determine the linear coefficients, we seek a solution to (3) that minimizes the difference between q and the filter input p . Specifically, we minimize the following cost function in the window:

$$(a_k, b_k) = \arg \min_{a, b} \sum_{i \in \omega_k} ((a I_i + b - p_i)^2 + \epsilon a^2). \text{----- (4)}$$

Here ϵ is a regularization parameter preventing ak from being too large. We will investigate its significance in Section 3.2. The solution to (4) can be given by linear regression [27]:

$$ak = \frac{1}{|\omega|} \sum_{i \in \omega_k} \omega_k l_i p_i - \mu_k^{-1} p_k \sigma_k^2 + \epsilon \quad (5)$$

$$bk = \frac{1}{|\omega|} p_k - ak \mu_k \quad (6)$$

Here, μ_k and σ_k^2 are the mean and variance of I in ω_k , $|\omega|$ is the number of pixels in ω_k , and $\frac{1}{|\omega|} p_k = \frac{1}{|\omega|} \sum_{i \in \omega_k} p_i$ is the mean of p in ω_k . Next we apply the linear model to all local windows in the entire image. However, a pixel i is involved in all the windows ω_k that contain i , so the value of q_i in (3) is not the same when it is computed in different windows. A simple strategy is to average all the possible values of q_i . So after computing (ak) for all patches ω_k in the image, we compute the filter output by:

$$q_i = \frac{1}{|\omega|} \sum_{k: i \in \omega_k} (ak l_i + bk) \quad (7)$$

Where $\frac{1}{|\omega|} a_i = \frac{1}{|\omega|} \sum_{k \in \omega_i} a_k$ and $\frac{1}{|\omega|} b_i = \frac{1}{|\omega|} \sum_{k \in \omega_i} b_k$. With this modification ∇q is no longer scaling of ∇I , because the linear coefficients $(\frac{1}{|\omega|} a_i, \frac{1}{|\omega|} b_i)$ vary spatially. But since $(\frac{1}{|\omega|} a_i, \frac{1}{|\omega|} b_i)$ are the output of an average filter, their gradients should be much smaller than that of I near strong edges. In this situation we can still have $\nabla q \approx \frac{1}{|\omega|} a \nabla I$, meaning that abrupt intensity changes in I can be mostly maintained in q . We point out that the relationship among I , p , and q given by (5), (6), and (8) are indeed in the form of image filtering (1). In fact, ak in (5) can be rewritten as a weighted sum of p : $ak = \sum_j (I) p_j$, where

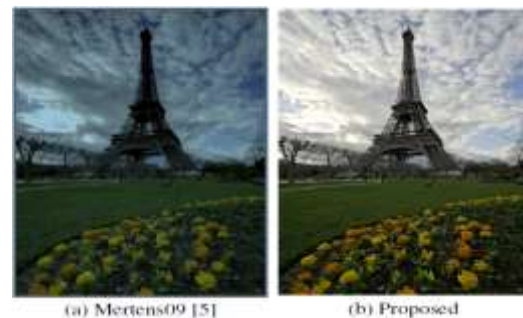
A_{ij} are the weights only dependent on I . For the same reason, we also have $b_k = \sum_j (I) p_j$ from (6) and $q_i = \sum_j W_{ij} (I) p_j$ from (8). It can be proven (see the supplementary materials) that the kernel weights can be explicitly expressed by:

$$W_{ij} (I) = \frac{1}{|\omega|} \sum_{k: (i,j) \in \omega_k} \frac{1}{1 + (I_i - \mu_k)(I_j - \mu_k) \sigma_k^2 + \epsilon} \quad (9)$$

Some further computations show that $\sum_j (I) = 1$. No extra effort is needed to normalize the weights.

4. EXPERIMENTAL RESULTS

Comparison of the proposed method with Mertens09 [5]. Source sequence by courtesy of Jacques Joffre. Cloud areas are much better preserved. Also, the colour appearance of the sky and the meadow regions is more natural and consistent with the source sequence.



5. CONCLUSION

MEF is a handy and practical image enhancement framework that is widely adopted in consumer electronics. Most existing MEF algorithms are pixel-wise methods, which often suffer from noisy weight maps. As a result, ad-hoc pre/post

processing steps are often involved in order to produce reasonable results. By contrast, the proposed method works with colour image patches directly by decomposing them into three conceptually independent components and determining each component respectively based on patch strength and exposedness measures. Experiments demonstrate that the proposed method produces compelling fused images both visually and in terms of a recently proposed objective quality model

Hybrid combination of DWT soft thresholding and guided filter is proposed to de-noise the medical images suffered with speckle noise. The proposed method results show excellence performances. In this paper compare the results in different variance with DWT, guided filter individually and guided + soft thresholding combinations performances

5. REFERENCES

- [1] E. Reinhard, W. Heidrich, P. Debevec, S. Pattanaik, G. Ward, and K. Myszkowski, High Dynamic Range Imaging: Acquisition, Display, and Image-based Lighting. Morgan Kaufmann, 2010.
- [2] M. Song, D. Tao, C. Chen, J. Bu, J. Luo, and C. Zhang, "Probabilistic exposure fusion," IEEE TIP, 2012.
- [3] P. J. Burt, The pyramid as a structure for efficient computation. Springer, 1984.
- [4] P. J. Burt and R. J. Kolczynski, "Enhanced image capture through fusion," in ICCV, 1993.
- [5] T. Mertens, J. Kautz, and F. Van Reeth, "Exposure fusion: A simple and practical alternative to high dynamic range photography," Computer Graphics Forum, 2009.
- [6] C. Tomasi and R. Manduchi, "Bilateral filtering for gray and color images," in ICCV, 1998.
- [7] K. He, J. Sun, and X. Tang, "Guided image filtering," in ECCV, 2010.
- [8] E. S. Gastal and M. M. Oliveira, "Domain transform for edge-aware image and video processing," ACM TOG, 2011.
- [9] S. Raman and S. Chaudhuri, "Bilateral filter based compositing for variable exposure photography," in Proc. Eurographics, 2009.
- [10] S. Li, X. Kang, and J. Hu, "Image fusion with guided filtering," IEEE TIP, 2013.
11. Petschnigg, G., Agrawala, M., Hoppe, H., Szeliski, R., Cohen, M., Toyama, K.: Digital photography with flash and no-flash image pairs. SIGGRAPH (2004)
12. Durand, F., Dorsey, J.: Fast bilateral filtering for the display of high-dynamic-range images. SIGGRAPH (2002)

13. Bae, S., Paris, S., Durand, F.: Two-scale tone management for photographic look. SIGGRAPH (2006)
14. Paris, S., Durand, F.: A fast approximation of the bilateral filter using a signal processing approach. ECCV (2006)
15. Porikli, F.: Constant time $o(1)$ bilateral filtering. CVPR (2008)
16. Yang, Q., Tan, K.H., Ahuja, N.: Real-time $o(1)$ bilateral filtering. CVPR (2009)
17. Adams, A., Gelfand, N., Dolson, J., Levoy, M.: Gaussian kd-trees for fast high dimensional filtering. SIGGRAPH (2009)